Carotid arteries segmentation in CT images with use of a right generalized cylinder model

Release 1.00

Leonardo Flórez Valencia[1], Jacques Azencot[2] and Maciej Orkisz[2]

July 21, 2009

[1]Pontificia Universidad Javeriana, Departamento de Ingeniería de Sistemas, Bogotá, Colombia; florez-l@javeriana.edu.co

[2]Université de Lyon; Université Lyon 1; INSA-Lyon; CNRS UMR5220; INSERM U630; CREATIS, F-69621 Villeurbanne, France; maciej.orkisz@creatis.insa-lyon.fr

Abstract

The arterial lumen is modeled by a spatially continuous right generalized cylinder with piece-wise constant parameters. The method is the identifies the parameters of each cylinder piece from a series of planar contours extracted along an approximate axis of the artery. This curve is defined by a minimal path between the artery end-points. The contours are extracted by use of a 2D Fast Marching algorithm. The identification of the axial parameters is based on a geometrical analogy with piece-wise helical curves, while the identification of the surface parameters uses the Fourier series decomposition of the contours. Thus identified parameters are used as observations in a Kalman optimal estimation scheme that manages the spatial consistency from each piece to another. The method was was evaluated on 15 training and 31 testing datasets from the MICCAI 3D Segmentation in the Clinic Grand Challenge: Carotid Bifurcation Lumen Segmentation and Stenosis Grading (http://cls2009.bigr.nl/).

Latest version available at the Insight Journal [http://hdl.handle.net/10380/3106]

Contents

Although healthy blood-vessels have cylindrical shapes with circular cross-sections, pathologies may lead to complex deformations of the cross-sectional shape. A generalized cylinder model capable of representing complex elongated objects, using a reduced number of parameters, was proposed in [1]. The model is composed of two parts: the first one describing the axial shape by means of orthonormal bases attached to the axis, and the second one describing the surface by means of contours in the planes orthogonal to the axis. This model was called RGC-sm, which stands for right generalized cylinder state model, since the authors used the system-state formalism. According to this formalism, both components (the local base and the cross-sectional contour) corresponding to any arc-length location, can be calculated knowing only one initial base and contour, as well as their dynamics (parameters describing their variation).

In this paper, we describe an implementation of this model for the purpose of carotid arteries segmentation and stenosis quantification. An early version of this work was published in [3].

1 Right generalized cylinder model

The RGC-sm model is an association of a generating curve $\mathcal{H}$ and a stack of contours describing the surface $\mathcal{S}$. The model is piecewise, *i.e.* it assumes that a generalized cylinder can be subdivided into pieces such that the model parameters be constant within each piece separately. Each piece $\mathcal{H}_i$ of the generating curve is defined by its length Δ_i, curvature κ_i, torsion τ_i and by the azimuthal rotation angle ν_i of the local basis $\Gamma_i(t)$ attached to $\mathcal{H}_i$, with respect to the corresponding Frenet frame. Each piece $\mathcal{S}_i$ of the surface is a continuous stack of contours $\mathbf{c}_i(t,\omega)$ defined by a tuple $\{\mathbf{Z}_i,\Lambda_i\}$, where $\mathbf{Z}_i = \{z_{i,l} \in \mathbb{C}; -q \leq l \leq +q\}$ represents the Fourier coefficients describing the first contour in the piece, and $\Lambda_i = \{\lambda_{i,l} \in \mathbb{C}; -q \leq l \leq +q\}$ is an ordered set of $2q+1$ coefficients linearly transforming the contour along $\mathcal{H}_i$:

$$\mathbf{c}_i(t,\omega) = \sum_{l=-q}^{+q} (\lambda_{i,l}(t-t_i) + z_{i,l}) e^{jl\omega}, \tag{1}$$

where t and ω respectively are arc-length and azimuthal parameters. The number q of harmonics controls the level of details of the contours, and thus of the whole generalized cylinder surface. Each surface piece $\mathcal{S}_i$ is connected to the corresponding generating curve piece $\mathcal{H}_i$ by the following equation:

$$\mathbf{s}_i(t,\omega) = \Gamma_i(t) \cdot \begin{bmatrix} 0 \\ \mathtt{Re}(\mathbf{c}_i(t,\omega)) \\ \mathtt{Im}(\mathbf{c}_i(t,\omega)) \end{bmatrix} + \mathbf{h}_i(t), \tag{2}$$

where $\mathbf{h}_i(t)$ is the spatial location of the origin of $\Gamma_i(t)$, which belongs to $\mathcal{H}_i$. The entire model is thus:

$$\mathcal{M} \equiv \{\mathbf{h}_0, \Gamma_0, \mathbf{Z}_0, \{\kappa_i, \tau_i, \nu_i, \Delta_i, \Lambda_i;\ 0 \leq i < n\}\}, \tag{3}$$

where $\mathbf{h}_0 \equiv \mathbf{h}_0(t=0)$ is the first point of $\mathcal{H}$, $\Gamma_0 \equiv \Gamma_0(t=0)$ is the first basis attached to $\mathbf{h}_0$ and $\mathbf{Z}_0 \equiv \mathbf{Z}_0(t=0)$ is the Fourier decomposition of the first RGC contour.

2 Kalman-based estimation of model parameters

Figure 1 shows the global flowchart of the proposed algorithm for vascular segmentation. The vascular segment of interest is delimited by two points interactively given by the user. The *Kalman state estimator* (KSE) [5] is used to control the vessel tracking along an approximate axis between these points. It predicts

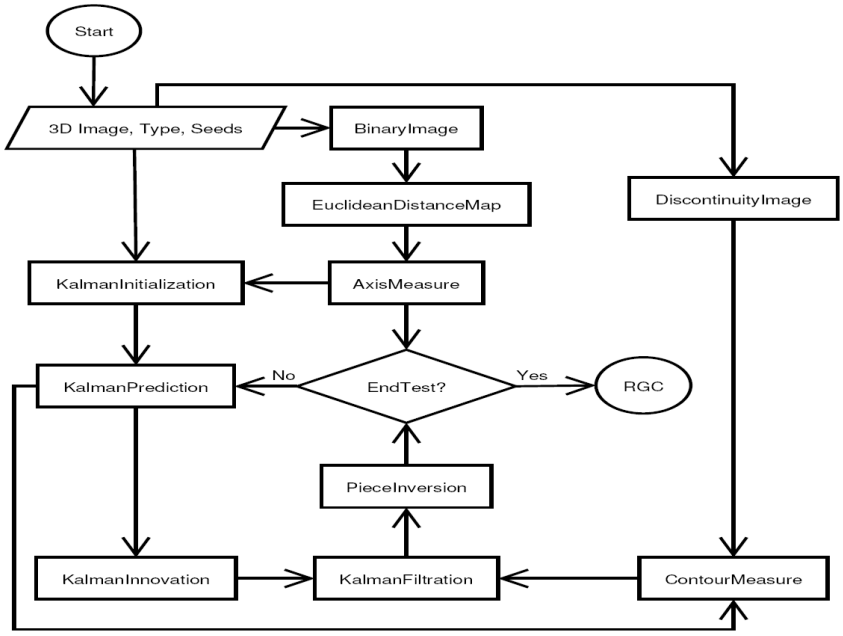

Figure 1: Flowchart of the segmentation algorithm.

the 3D locations, orientations and shapes of the contours that delimit the consecutive cylinder pieces. The observation vector, coding the RGC-sm parameters of the *i*-th piece, is computed from the result of the contour extraction performed in the predicted plane. The observation is then filtered by the KSE to produce a corrected estimate of the parameters, which is expected to smooth out the possible errors of the contours and initial axis extraction. Only the very first contour remains uncorrected.

The KSE adapts the tracking speed to the complexity of the local vascular shapes (axial and superficial). In complex shapes (high local changes of curvature, for example) the length of the cylinder piece is automatically reduced. This occurs when the predicted contours are too different from the observations.

3 Retrieval of observations from image data

Without loss of generality, we explain the process for the first cylinder piece. Under the assumption of constant curvature and torsion, each piece of $\mathcal{H}$ is a helix, and a geometrical reasoning demonstrates that its parameters can be recovered if the frames Γ_0, Γ_1 at its extremities, as well as their origin locations $\mathbf{h}_0$ and $\mathbf{h}_1$, are available. Owing to a lack of space here, this reasoning will be given in a future publication. The remaining parameters are calculated using the Fourier decompositions of the contours $\mathbf{Z}_0$ and $\mathbf{Z}_1$. We first give main equations that lead from Γ_0, Γ_1, $\mathbf{h}_0$, $\mathbf{h}_1$, $\mathbf{Z}_0$ and $\mathbf{Z}_1$ to the RGC-sm parameters. Then we explain the image processing steps that lead from the initial image and seed-points to these intermediate data.

Calculation of model parameters

We first compute the transition operators, respectively rotation and translation, between the extremities:

$$\Phi(0,\Delta_0) = \Gamma_0^\top \cdot \Gamma_1, \tag{4}$$

$$\mathbf{Tr}(0,\Delta_0) = \Gamma_0^\top \cdot (\mathbf{h}_1 - \mathbf{h}_0)\,. \tag{5}$$

Then, using the properties of the rotation matrices, we obtain some useful intermediate results:

$$\Phi(0,\Delta_0) - \Phi(0,\Delta_0)^\top = \begin{bmatrix} 0 & -c & b \\ c & 0 & -a \\ -b & a & 0 \end{bmatrix},$$

$$\Theta = \arcsin\left(\sqrt{a^2+b^2+c^2}/2\right),$$

$$\varphi = \arcsin\left(a/\sqrt{a^2+b^2+c^2}\right),$$

and a first output parameter:

$$\nu_0 = \arctan(b/c). \tag{6}$$

Now, the use of the properties of the helical curves leads to another intermediate result:

$$\mu = \frac{\sin\Theta\cos^2\varphi + \Theta\sin^2\varphi}{\left[\Phi(0,\Delta_0)\ \begin{bmatrix}1 & 0 & 0\end{bmatrix}^\top\ \right]^\top \mathbf{Tr}(0,\Delta_0)},$$

which in turn permits the computation of the remaining axial parameters:

$$\begin{cases} \kappa_0 &= \mu\cos\varphi, \\ \tau_0 &= \mu\sin\varphi, \\ \Delta_0 &= \Theta/\mu. \end{cases} \tag{7}$$

Numerical stability problems might arise when $\Phi(0,\Delta_0) = \mathbf{I}$, which occurs when $\mathcal{H}_0$ is a straight line segment. This is checked after the computation of Γ_0 and Γ_1, and the parameters, in this case, are set as follows: $\begin{bmatrix} \kappa_0 & \tau_0 & \nu_0 & \Delta_0 \end{bmatrix}^\top = \begin{bmatrix} 0 & 0 & 0 & |\mathbf{h}_1 - \mathbf{h}_0| \end{bmatrix}^\top$. The last step is the computation of the parameters describing the linear evolution of the Fourier decomposition of the contours:

$$\Lambda_0 = \left\{ \frac{z_{1,l} - z_{0,l}}{\Delta} \in \mathbb{C} : -q \le l \le +q \right\}. \tag{8}$$

Approximate axial shape extraction

As mentioned above, in the current implementation, the vessel tracking with Kalman estimation of RGC-sm parameters is performed along an initial approximate axis $\tilde{\mathcal{H}}$. The line $\tilde{\mathcal{H}}$, that coarsely describes the axial shape of the vessel, is constructed as follows:

1. A binary image $\mathcal{B}(\mathbf{p})$ is computed from the initial image $I(\mathbf{p})$, using locally adaptive thresholds that coarsely separate the vascular lumen from the background. These thresholds are defined using the results presented in [4]. According to that work, the vascular lumen intensities along the carotids have two properties: (a) the global lower threshold values are in the range [140HU, 420HU], and (b) the local threshold values vary almost linearly along the vessel axis. Using these properties, the lumen is segmented using a flooding algorithm that computes thresholds depending on the distance of each voxel to user-given seeds. The local threshold properties are computed using the Robust Automatic Threshold Selection (RATS) scheme [6].

2. An *Euclidean distance map* $\mathcal{E}(\mathbf{p})$ is computed within $\mathcal{B}(\mathbf{p})$ using the algorithm proposed in [7].

3. Finally, a cost function $\mathcal{F}(\mathbf{p}) = \frac{1}{1+\mathcal{E}(\mathbf{p})}$ is used for a *minimal path* algorithm (as proposed in [9]), which finds a set $\tilde{\mathcal{H}}$ of points ordered along the shape and connecting the seed-points even in the presence of lumen discontinuities (severe stenoses). These points are expected to be located near the center of the vessel due to the cost function $\mathcal{F}(\mathbf{p})$, related to the distance map $\mathcal{E}(\mathbf{p})$.

Contours extraction

The planar contours are extracted using the *fast marching* (FM) method [8]. FM is a *front propagation* technique that provides a set of (counter-clockwise) *ordered* points $\mathcal{C}_i = \{\mathbf{c}_{i,k} : 0 \leq k < K\}$. This technique needs the definition of a speed function $\mathcal{R}(\mathbf{p})$ expected to be minimum (~ 0) at discontinuities (edges) and maximum within uniform regions (~ 1). We use the speed function proposed in [2], where the native image intensities $I(\mathbf{p})$ along with image discontinuities represented by the gradient magnitude $|\nabla I(\mathbf{p})|$ are used. Instead of a direct use of $|\nabla I(\mathbf{p})|$, the proposed function uses exponential factors that strongly decrease the propagation speed when the front moves beyond local maxima of the gradient norm (i.e. beyond borders of the arteries) and beyond the range of luminal intensities, defined as described in previous subsection. Furthermore, in this work the authors recommend that the FM propagation should be stopped at time value T when the the growth of the area A encompassed by the front becomes very slow, which is characterized by a large value of $\Delta T/\Delta A$.

Front propagation is performed in the plane passing through the predicted point $\hat{\mathbf{h}}_i \in \tilde{\mathcal{H}}$, and oriented according to the predicted vessel orientation expressed by the orthogonal base $\hat{\Gamma}_i$. Summarizing, the point set $\mathcal{C}_i$ is extracted as follows:

1. The speed image $\mathcal{R}(\mathbf{p})$ is sliced by the plane passing by $\hat{\mathbf{h}}_i$ and oriented by the first column vector of $\hat{\Gamma}_i$, to obtain a 2D image $\mathcal{Q}_i(\mathbf{p})$.
2. The FM algorithm is executed on $\mathcal{Q}_i(\mathbf{p})$ with $\hat{\mathbf{h}}_i$ as the first trial point (front initialization).
3. The FM generates the level set $\mathcal{L}_i(\mathbf{p})$ which contains $\mathcal{C}_i$ as its last level.

The initialization of the RGC-sm reconstruction process requires $\mathbf{h}_0$, Γ_0 and $\mathbf{Z}_0$. One of the seed-points (typically the distal one) is taken as $\mathbf{h}_0$. The orthonormal basis Γ_0 is constructed such that its first vector is tangent to $\tilde{\mathcal{H}}$ in $\mathbf{h}_0$, the second vector is oriented along $\mathbf{h}_0 - \mathbf{c}_{0,0}$, and the third one is orthogonal to both. $\mathbf{Z}_0$ is calculated as the Fourier series corresponding to $\mathcal{C}_0$.

4 Results

Both lumen segmentation and stenosis quantification were evaluated on 15 training and 31 testing carotid CTA datasets available within the Carotid Bifurcation Algorithm Evaluation Framework. Details of the evaluation methodology can be found on the web page of the challenge (http://cls2009.bigr.nl/). Figure 2 displays an example of segmentation result.

Four criteria were evaluated to assess the lumen segmentation: Dice similarity index, mean surface distance, RMS surface distance and maximal surface distance. Tables 1 and 2 summarize the results obtained.

Stenosis quantification was evaluated by calculating the difference between the calculated percentage and the one provided by the reference standard, using both cross-sectional areas and diameters. The results are presented in Tables 3 and 4.

Table 1: Summary testing lumen

Measure	% / mm			rank		
	min.	max.	avg.	min.	max.	avg.
L_dice	0.0%	92.4%	51.8%	4	4	4.00
L_msd	0.32mm	14.91mm	3.42mm	4	4	4.00
L_rmssd	0.55mm	15.53mm	4.29mm	4	4	4.00
L_max	1.28mm	17.50mm	9.46mm	4	4	4.00
Total (lumen)				**4**	**4**	**4.00**

Table 2: Averages testing lumen

Team name	Total success	dice		msd		rmssd		max		Total rank
		%	rank	mm	rank	mm	rank	mm	rank	
Our method	29	51.8	4.0	3.42	4.0	4.29	4.0	9.46	4.0	4.0
ObserverA	31	95.4	1.5	0.10	1.6	0.13	1.7	0.56	2.0	1.7
ObserverB	31	94.8	2.4	0.11	2.4	0.15	2.4	0.59	1.8	2.2
ObserverC	31	94.7	2.2	0.11	2.2	0.15	2.2	0.71	2.4	2.2

5 Discussion and conclusion

RGC-sm is a powerful tool that permits a concise description of complex generalized cylindrical shapes. The theoretical framework permits the reconstruction of a continuous surface corresponding to the lumen, based on a limited number of discrete contours. Additionally, the Kalman estimator permits a correction of the observation errors when these remain within a reasonable range. However, our current implementation of the image processing steps devised to provide the observations is clearly not optimal. The initial rough extraction of the axial shape begins by a thresholding step, which is prone to errors when neighboring structures have a similar intensity range. Actually, this initial curve needs to be quite well-centered within the lumen. Indeed, as the Fast Marching algorithm in planes orthogonal to this initial curve starts from the intersection between the plane and the curve, this intersection has to fall within the lumen, otherwise the contour extraction fails. Failures are also observed when the curve is located within the lumen, close to a poorly contrasted boundary. In fact, the use of an always inflating deformable contour, such as the Fast Marching front, is uneasy, since the speed function and stopping criteria hardly can cope with all possible configurations (nearby veins, calcifications, etc.). Furthermore, 2D Fast Marching does not exploit the 3D continuity of the vascular lumen, which might be helpful in some complicated situations. Future work will be oriented towards an implementation that do not require the initial extraction of an approximate axial shape and that perform a piece-wise local 3D boundary extraction. Let us also note that the current implementation was designed with an implicit assumption that the seed-points are given at "easy" locations, *i.e.* healthy circular cross-sections without neighboring structures "stuck" to the artery of interest, and that the seed-points can also be considered as end-points. However, in several testing datasets the seed-point in the internal carotid artery was located either too close to the bifurcation, so that our method segmented a too short part of the artery, or far within the skull where the assumption of the absence of neighboring structures did not hold.

Acknowledgements

This work has been partly supported by by Région Rhône-Alpes project PP3/I3M and by the internal project 2077 "Vitral 3" at the Pontificia Universidad Javeriana.

Table 3: Summary testing stenosis

Measure	%			rank		
	min.	max.	avg.	min.	max.	avg.
S_area	0.0%	100.0%	32.8%	1	4	3.32
S_diam	0.0%	100.0%	40.3%	1	4	3.39
Total (stenosis)				**1**	**4**	**3.35**

Table 4: Averages testing stenosis

Team name	Total success	area		diam		Total rank
		%	rank	%	rank	
Our method	31	32.76	3.3	40.31	3.4	3.4
ObserverA	31	2.71	1.3	3.61	1.5	1.4
ObserverB	31	4.55	1.6	5.29	1.7	1.7
ObserverC	31	5.61	2.2	5.74	1.9	2.1

References

[1] J. Azencot and M. Orkisz. Deterministic and stochastic state model of right generalized cylinder (RGC-sm): application in computer phantoms synthesis. *Graph. Models*, 65(6):323–350, 2003. (document)

[2] M. Baltaxe Milwer, L. Flórez Valencia, M. Hernández Hoyos, I.E. Magnin, and M. Orkisz. Fast marching contours for the segmentation of vessel lumen in CTA cross-sections. In *Conf Proc IEEE Eng Med Biol Soc*, pages 791–794, Lyon, France, 2007. IEEE, IEEE. 3

[3] L. Flórez Valencia, J. Azencot, F. Vincent, M. Orkisz, and I.E. Magnin. Segmentation and Quantification of Blood Vessels in 3D Images using a Right Generalized Cylinder State Model. In *Proc. IEEE International Conference on Image Processing*, pages 2441–2444, 2006. (document)

[4] L. Flórez Valencia, F. Vincent, and M. Orkisz. Fast 3D pre-segmentation of arteries in computed tomography angiograms. In *Int. Conf. Comput. Vision & Graphics*, pages 87–88, Warsaw, Poland, 2004. 1

[5] R.E. Kalman. A New Approach to Linear Filtering and Prediction Problems. *Transactions of the ASME–Journal of Basic Engineering*, 82(Series D):35–45, 1960. 2

[6] Josef Kittler, John Illingworth, and J. Fglein. Threshold selection based on a simple image statistic. *Computer Vision, Graphics, and Image Processing*, 30(2):125–147, 1985. 1

[7] Calvin R. Maurer, Jr., Rensheng Qi, and Vijay Raghavan. A linear time algorithm for computing exact euclidean distance transforms of binary images in arbitrary dimensions. *IEEE Trans. Pattern Anal. Mach. Intell.*, 25(2):265–270, 2003. 2

[8] J.A. Sethian. A Fast Marching Level Set Method for Monotonically Advancing Fronts. In *Proc. Nat. Acad. Sci.*, volume 93, pages 1591–1595, 1996. 3

[9] O. Wink, W.J. Niessen, A.F. Frangi, B. Verdonck, and M.A. Viergever. 3D MRA coronary axis determination using a minimum cost path approach. *Magnetic Resonance in Medicine*, 47(6):1169–1175, 2002. 3

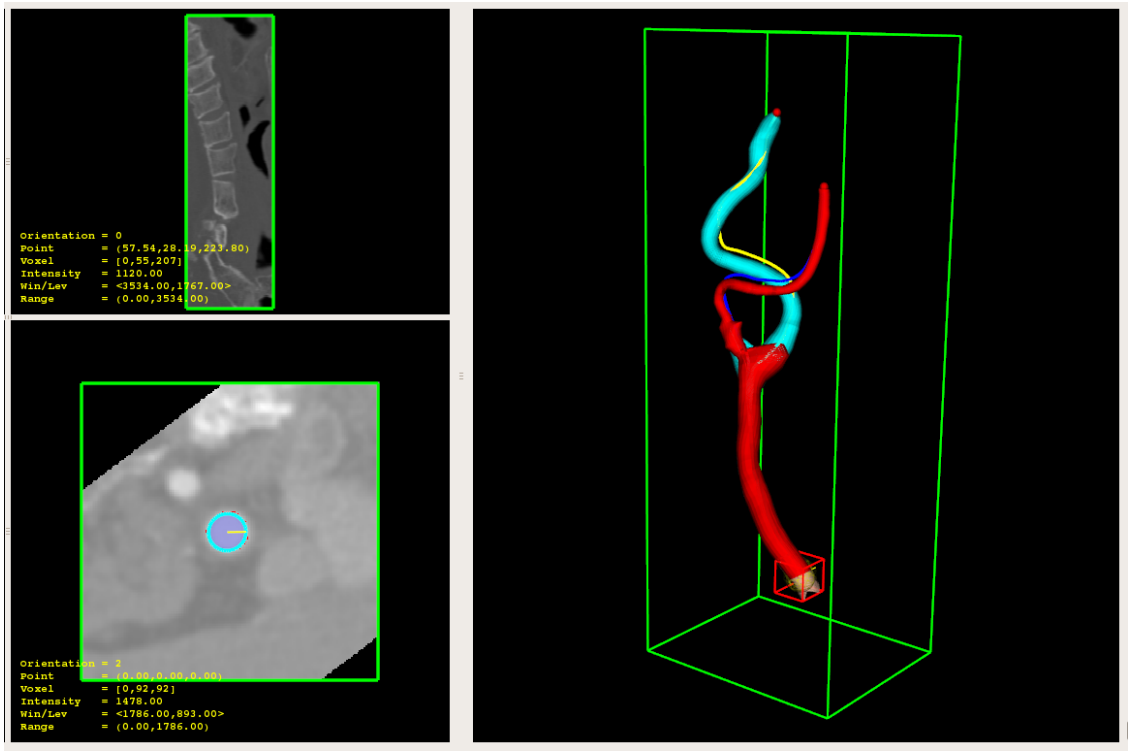

Figure 2: Example of the segmentation of a CTA image of a carotid using our algorithm. The internal carotid is presented in cyan and the external carotid is presented in red. The yellow and blue lines represent the generating curves calculated.